Supplementary Material

Control of the serine integrase reaction: roles of the coiled-coil and helix E regions in DNA site synapsis and recombination

Mandali and Johnson

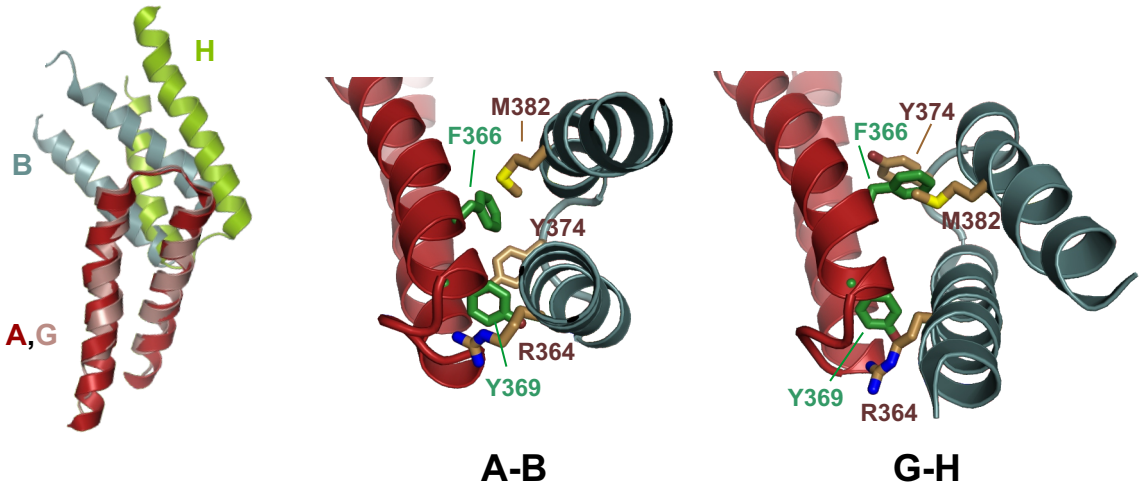

FIGURE S1 The CC motif tip interfaces viewed in a different orientation than in Fig. 5A to highlight select differences between CC pairs A-B and G-H in PDB code 5U96. The two CC pair structures are aligned over the A and G chains as shown in the left panel.

The positions of the Tyr374 side chain in the two pairs are radically different; Int-Y374A exhibits little *PB* but moderate *LR* recombination. Int-F366A, and M382A exhibit more robust *LR* than *PB* recombination; F366A and F366K exhibit weak *LR* recombination in vitro without Gp44. Int-R364A and Y369A are severely defective for both *PB* and *LR* recombination.

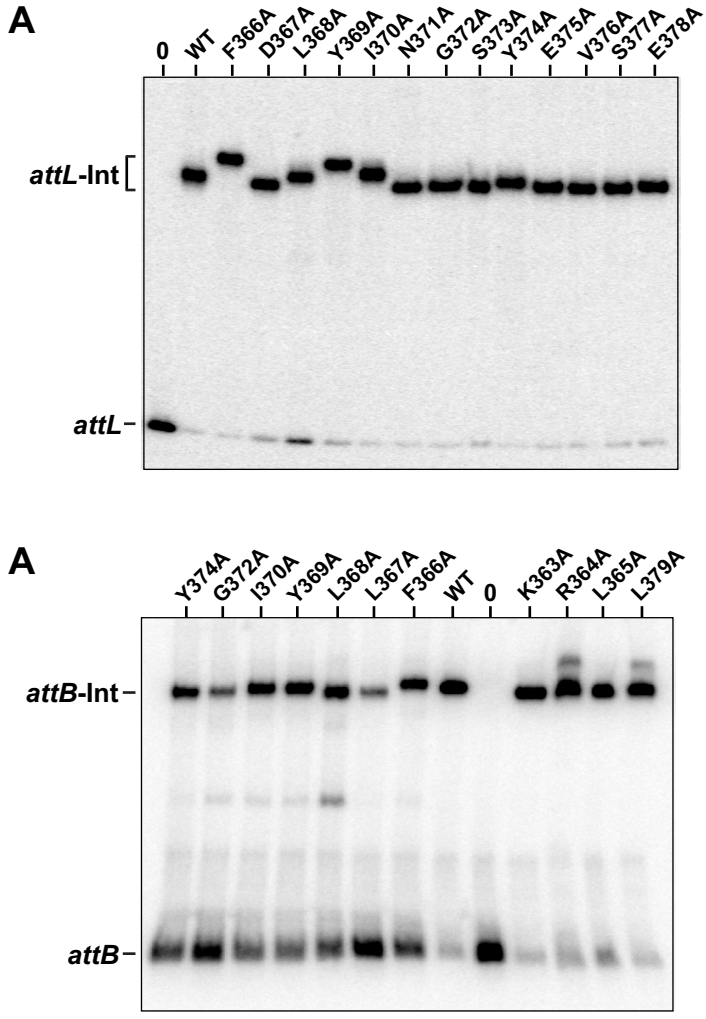

FIGURE S2. Electrophoretic migrations of CC alanine mutants bound at (A) *attL* and (B) *attB* through 59:1 polyacrylamide:bisacrylamide gels, which enhance migration differences. Little migration differences are observed with *attB* complexes, with the possible exception of slightly slower mobility by F366A.

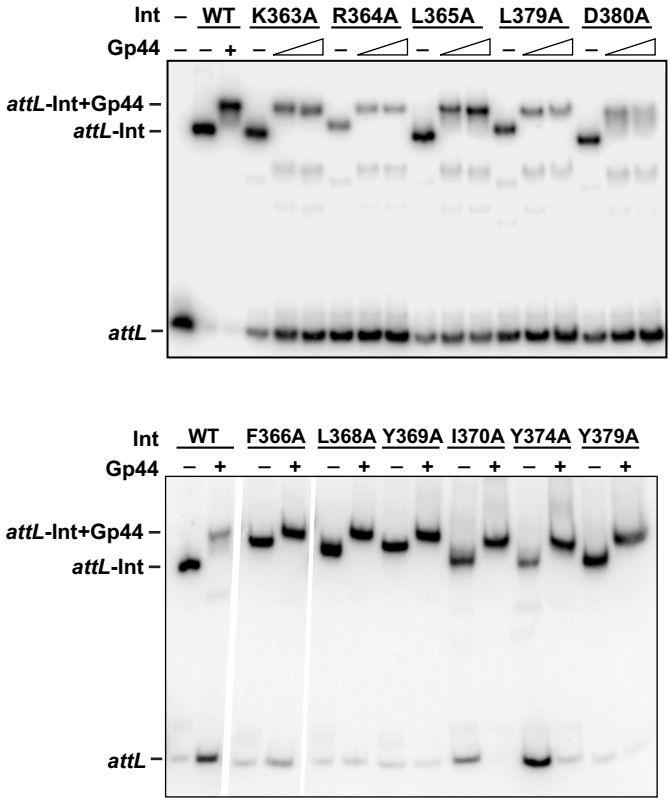

FIGURE S3. Int CC mutants bound to *attL* exhibit the same electrophoretic mobilities upon Gp44 binding.

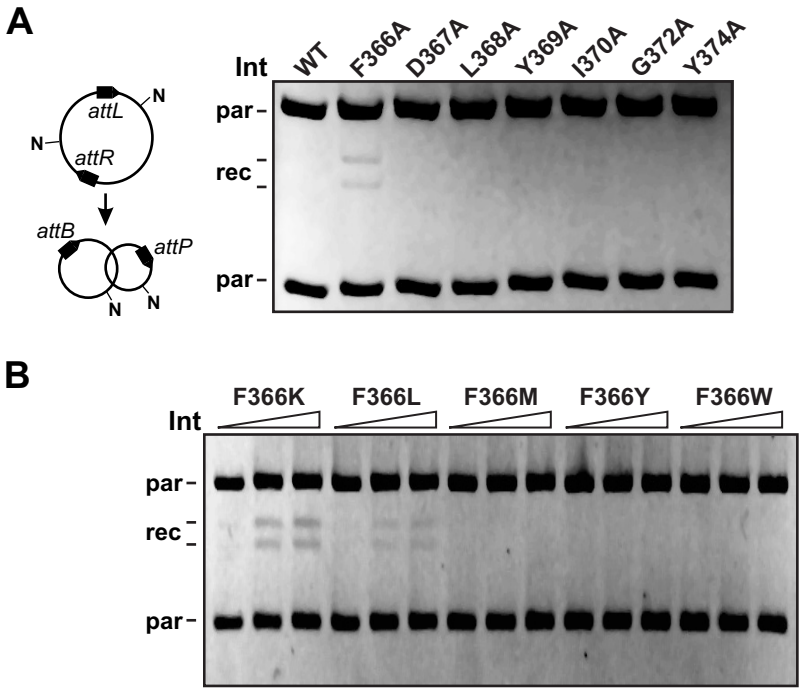

FIGURE S4. Gp44-independent *attL* x *attR* recombination by CC tip alanine mutants.
(A) *attL* x *attR* deletion reactions were performed for 20 min without Gp44, and the products digested with Nde I before electrophoresis (schematic on left). Of the alanine-substitution set between Int residues 362-383 only Int-F366A gave detectable recombinant products.
(B) Different amino acid substitutions at residue 366 were evaluated for Gp44-independent *attL* x *attR* recombination as in panel A. Two-fold increasing concentrations of Int mutants were added to the reaction. The low level reaction by Int-F366K was similar to that of F366A.

FIG S5A

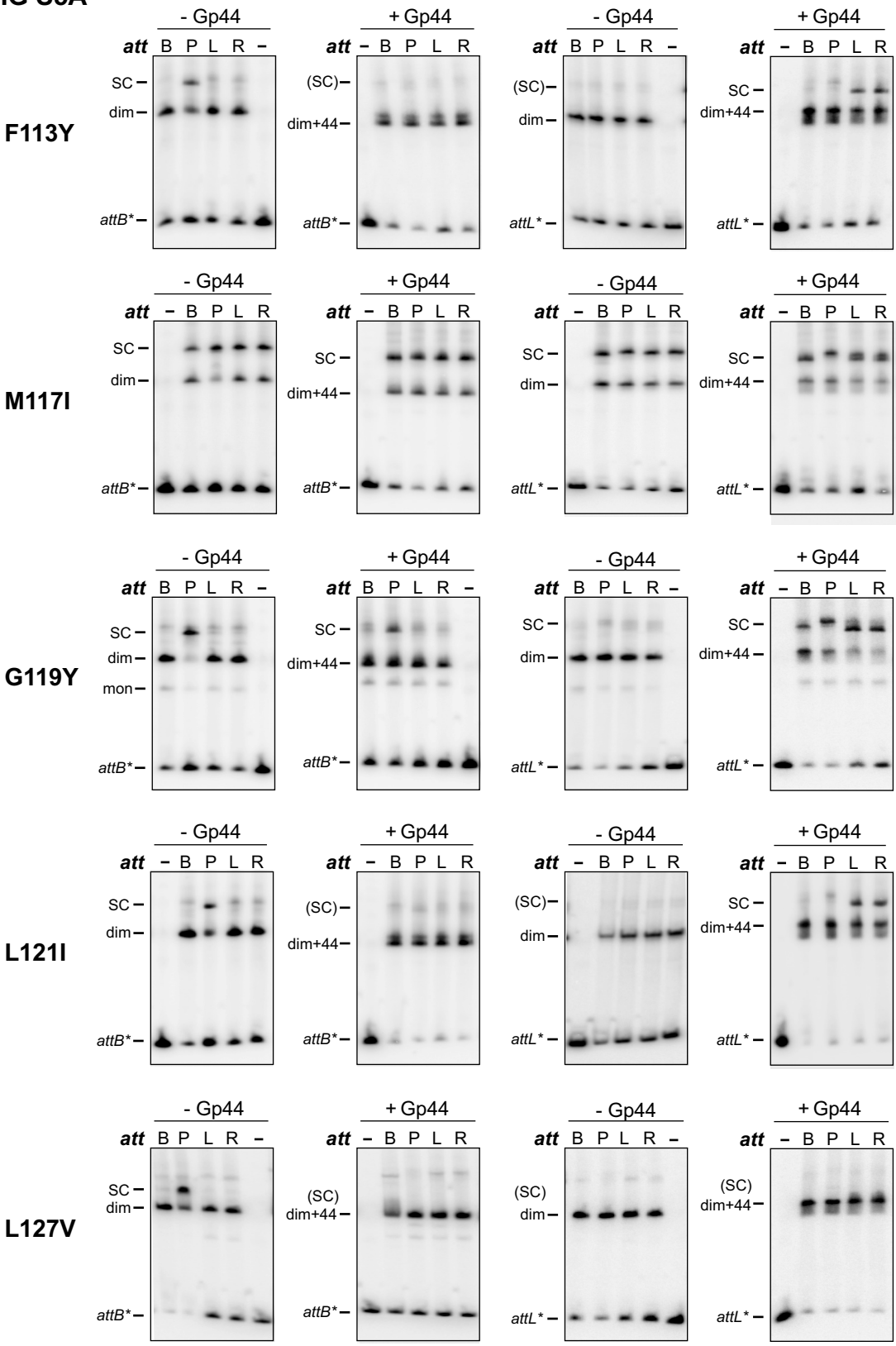
F113Y
M117I
G119Y
L121I
L127V
- Gp44
+ Gp44
att
B P L R –
– B P L R
SC
(SC)
dim
dim+44
mon
attB*
attL*

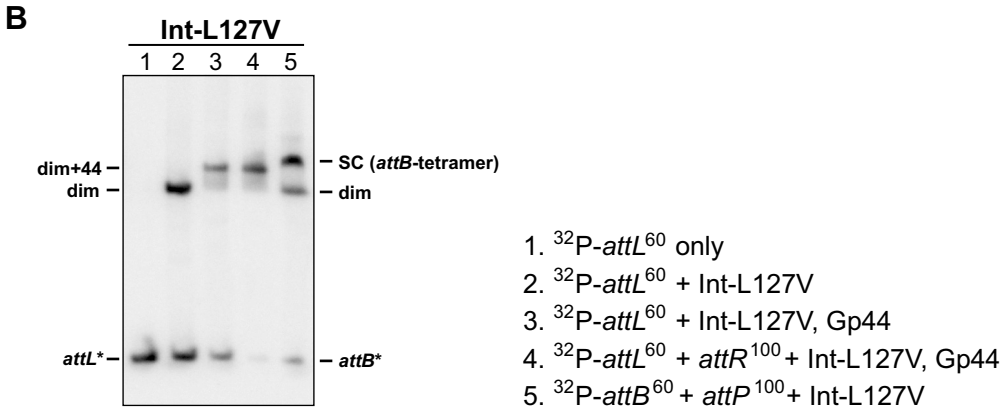

FIGURE S5. Specificity of *att* site synapsis by A118 helix E mutants.
(A) Each of the helix E mutants are assayed for SC formation with labeled 60 bp *attB* or *attL* and excess unlabeled 100 bp fragments of each *att* site in the absence or presence of Gp44. The locations of the unbound labeled *attB** or *attL** probe, the Int dimer complex (dim), Int dimer +Gp44 (dimer+44), and synaptic complex (SC) bands (if present) are denoted. Note that Gp44 binding shifts Int dimers bound to *attB* and *attL* to faster and slower migrating complexes, respectively. A small amount of DNA-bound monomeric (mon) Int-G119Y is present. For Int-M117I, the SCs whose formation is expected to be augmented by CC interactions (BP and Gp44-activated LL and LR) were present at the highest levels. CC-dependent synapsis by two *attL* sites, which would be expected to align in an antiparallel configuration, would not be expected to support recombination because the core nucleotides would be incompatible with ligation after subunit rotation (13). All gels were 37.5:1 acrylamide:bisacrylamide.

(B) Formation of LR SCs (**attL*-Int tetramer) by Int-L127V is not evident. Reactions loaded on each lane are given to the right of the gel; the **attB* x *attP* reaction in lane 5 shows that the migration of the BP SC (**attB*-Int tetramer) is slightly slower than the Gp44-bound Int-L127V dimer complexed with **attL*. Gel was 59:1 acrylamide:bisacrylamide.

TABLE S1. Plasmids used in this study.

Plasmid	Description	Source
pRJ2184	pET15b, A118 integrase (*gp31*) between NdeI and BamH1	(1)
pGV2710	pETDuet-derived with A118 *gp44*+intein^{Mxe}-6His tag	(2)
pRJ2214	pBR322, *attP* (400 bp) into EcoR1	(1)
pRJ2215	pBR322, *attB* (200 bp) into Sal1	(1)
pRJ2191	pBR322, *attL* (200 bp) between EcoR1-SalI	(2)
pRJ2193	pBR322, *attR* (200 bp) between EcoR1-SalI	(2)
pRJ2986	pBR322, *amp* DR[1](*attL-lacZ-attR*)	(2)
pRJ3244	pBR322, *amp* DR(*attB-lacZ-attP*)	(2)
pRJ3193	pUC18, *attB*>*L* (Fig. 2A) into SmaI	This work
pRJ3194	pUC18, *attB*>*L* (Fig. 2A) into SmaI	This work
pRJ3195	pUC18, *attP*>*L* (Fig. 2A) into SmaI	This work
pRJ3196	pUC18, *attP*>*R* (Fig. 2A) into SmaI	This work
pRJ3231	pUC18, *attB*>*P* (Fig. 2A) into SmaI	This work
pRJ3232	pUC18, *attP*>*B* (Fig. 2A) into SmaI	This work
pRJ3532	pRJ2184 *int*Δ(350-356)[2]	This work
pRJ3533	pRJ2184 *int*Δ(350-356, 391-397) [CCΔ7 in Fig. 4]	This work
pRJ3534	pRJ2184 *int*-TP*901*(350-356, 391-397) [CC chimera in Fig. 4]	This work
pRJ3535	pRJ2184 *int* with two 7 residue insertions in CC motif [CC+7 in Fig. 4]	This work
pRJ3536-57	pRJ2184 *int* with CC alanine substitutions between 362 and 383	This work
pRJ3402	pRJ2184 *int*-F113Y	This work
pRJ3403	pRJ2184 *int*-M117I	This work
pRJ3404	pRJ2184 *int*-G119Y	This work
pRJ3405	pRJ2184 *int*-L121I	This work
pRJ3406	pRJ2184 *int*-L127V	This work
pRJ3259	pRJ2184, *int* ΔCC(342-416)	(2)
pRJ3408	pRJ3259 *int*-F113Y ΔCC(342-416)	This work
pRJ3409	pRJ3259 *int*-M117I ΔCC(342-416)	This work
pRJ3410	pRJ3259 *int*-G119Y ΔCC(342-416)	This work
pRJ3411	pRJ3259 *int*-L121I ΔCC(342-416)	This work
pRJ3412	pRJ3259 *int*-L127V ΔCC(342-416)	This work

[1] DR indicates *att* sites in direct repeat orientation.

[2] Int amino acid residues are listed.

References

1. Mandali S, Dhar G, Avliyakulov NK, Haykinson MJ, Johnson RC. 2013. The site-specific integration reaction of *Listeria* phage A118 integrase, a serine recombinase. Mobile DNA 4:2. https://doi.org/10.1186/1759-8753-4-2.

2. Mandali S, Gupta K, Dawson AR, Van Duyne GD, Johnson RC. 2017. Control of recombination directionality by the *Listeria* phage A118 protein Gp44 and the coiled-coil motif of its serine integrase. J Bacteriol 199:e00019-17.